z Expansion and Nucleon Vector Form Factors

GENIE z Expansion Workshop
Fermilab, Batavia, IL

Gabriel Lee

Technion – Israel Institute of Technology
ongoing work with J. Arrington, R. Hill, Z. Ye

Sep 1, 2016

Form Factors and ep Scattering

- Mott cross-section for scattering of a relativistic electron off a recoiling point-like nucleus is

$$\left(\frac{d\sigma}{d\Omega}\right)_M = \frac{Z^2\alpha^2}{4E^2\sin^4\frac{\theta}{2}}\cos^2\frac{\theta}{2}\frac{E'}{E}\,.$$

- The Rosenbluth formula generalizes the above,

$$\left(\frac{d\sigma}{d\Omega}\right)_R = \left(\frac{d\sigma}{d\Omega}\right)_M \frac{1}{1+\tau}\left[G_E^2 + \frac{\tau}{\epsilon}G_M^2\right],\ \tau = \frac{-q^2}{4M^2},\ \epsilon = \frac{1}{1+2(1+\tau)\tan^2\frac{\theta}{2}}.$$

- The Sachs form factors $G_E(q^2), G_M(q^2)$ account for the finite size of the nucleus. In terms of the standard Dirac (F_1) and Pauli (F_2) form factors,

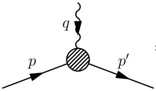

$$= \Gamma^\mu(q^2) = \underbrace{\frac{G_E+\tau G_M}{1+\tau}}_{F_1(q^2)}\gamma^\mu + \frac{i}{2M}\sigma^{\mu\nu}q_\nu \underbrace{\frac{G_M - G_E}{1+\tau}}_{F_2(q^2)}\,.$$

- The form factors are normalized at $q^2 = 0$ to the charge and anomalous magnetic moments, e.g., for the proton,

$$G_E^p(0) = 1, G_M^p(0) = \mu_p.$$

- Quantities like the charge radius and the form factor curvature are defined by derivatives of G evaluated at $q^2 = 0$, e.g.,

$$\langle r^2\rangle \equiv \frac{6}{G(0)}\frac{\partial G}{\partial q^2}\bigg|_{q^2=0}.$$

Earlier Ansäntze for G_E, G_M

$$\left(\frac{d\sigma}{d\Omega}\right)_R = \left(\frac{d\sigma}{d\Omega}\right)_M \frac{1}{1+\tau}\left[G_E^2 + \frac{\tau}{\epsilon} G_M^2\right]$$

- Previous analyses used simple functional forms for G_E, G_M, with expansions truncated at some finite k_{max}:

$$G_{\text{poly}}(q^2) = \sum_{k=0}^{k_{\text{max}}} a_k (q^2)^k \,,$$ polynomials, Simon et al. (1980), Rosenfelder (2000)

$$G_{\text{invpoly}}(q^2) = \frac{1}{\sum_{k=0}^{k_{\text{max}}} a_k (q^2)^k} \,,$$ inverse polynomials, Arrington (2003)

$$G_{\text{cf}}(q^2) = \frac{1}{a_0 + a_1 \frac{q^2}{1 + a_2 \frac{q^2}{1+\dots}}} \,,$$ continued fractions, Sick (2003)

- Hill & Paz (2010) showed that the above functional forms exhibit pathological behaviour with increasing k_{max}.
- Other, more complicated functional forms exist, see, e.g., Bernauer et al. (2014).

The Bounded z Expansion

- For the proton, QCD constrains the form factors to be analytic in $t \equiv q^2 \equiv -Q^2$ outside of a time-like cut beginning at $t_{\text{cut}} = 4m_\pi^2$, the two-pion production threshold. Clearly this presents an issue with convergence for expansions in the variable q^2. Hill & Paz (2010)
- Using a conformal map, we obtain a true small-expansion variable z for the physical region:

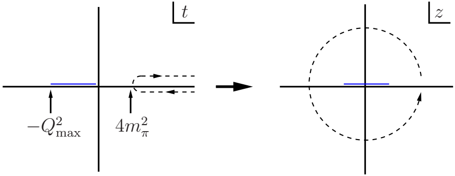

$$z(t; t_{\text{cut}}, t_0) = \frac{\sqrt{t_{\text{cut}} - t} - \sqrt{t_{\text{cut}} - t_0}}{\sqrt{t_{\text{cut}} - t} + \sqrt{t_{\text{cut}} - t_0}}$$

$$G_E = \sum_{k=0}^{k_{\text{max}}} a_k [z(q^2)]^k \,, \quad G_M = \sum_{k=0}^{k_{\text{max}}} b_k [z(q^2)]^k \,.$$

- The physical kinematic region of scattering experiments lies on the negative real line. For a set of data with a maximum momentum transfer Q^2_{max}, this is represented by the blue line.
- The conformal map has a parameter t_0, which is the point in t plane that is mapped to $z(t_0) = 0$.
- By including other data, such as from $\pi\pi \to N\bar{N}$ or eN scattering, it is possible to move the t_{cut} to larger values, improving the convergence of the expansion.

More on t_0

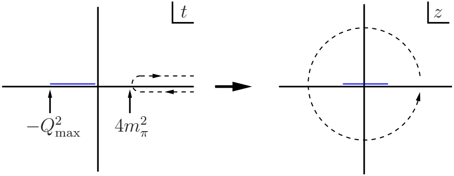

$$z(t; t_{\text{cut}}, t_0) = \frac{\sqrt{t_{\text{cut}} - t} - \sqrt{t_{\text{cut}} - t_0}}{\sqrt{t_{\text{cut}} - t} + \sqrt{t_{\text{cut}} - t_0}}$$

- Since the conformal mapping is an analytic function, on the closed set $t \in [-Q^2_{\text{max}}, 0]$, it attains a maximum $|z_{\text{max}}|$ at one of the endpoints $t = 0$ or $t = -Q^2_{\text{max}}$.
- We can find an optimal choice t_0^{opt} to minimize this value $|z_{\text{max}}|$,

$$t_0^{\rm opt}(Q^2_{\rm max}) = t_{\rm cut}\left(1 - \sqrt{1 + Q^2_{\rm max}/t_{\rm cut}}\right) \quad \Rightarrow \quad |z|^{\rm opt}_{\rm max} = \frac{(1 + Q^2_{\rm max}/t_{\rm cut})^{\frac{1}{4}} - 1}{(1 + Q^2_{\rm max}/t_{\rm cut})^{\frac{1}{4}} + 1}.$$

- Choosing an appropriate t_0 can make a big difference on the required k_{max} for convergence; below $n_{\rm min}$ is such that $|z|^{n_{\rm min}} < 0.01$.

$Q^2_{\rm max}$ [GeV^2]	t_0 [GeV^2]	$\lvert z\rvert_{\rm max}$	$n_{\rm min}$
1	0	0.58	8.3
1	$t_0^{\rm opt}(1\,{\rm GeV}^2) = -0.21$	0.32	4.0
3	0	0.72	14
3	$t_0^{\rm opt}(3\,{\rm GeV}^2) = -0.41$	0.43	5.4

Sum Rules from Large Q^2 Behaviour

- QCD also demands that the form factor fall off faster than $1/Q^4$ up to logs as $Q^2 \to \infty$ (dipole-like behaviour),

$$Q^n G(-Q^2)\Big|_{Q^2\to\infty} \to 0 \quad \Rightarrow \quad \frac{d^n G}{dz^n}\Big|_{z\to 1} \to 0, \quad n = 0, 1, 2, 3,$$

- For a form factor employing the z expansion truncated at some k_{max}, we can enforce this by implementing four sum rules, Lee, Arrington, Hill (2015)

$$\sum_{k=1}^{k_{\text{max}}} k(k-1)\cdots(k-n+1)a_k = 0, \quad n = 0, 1, 2, 3.$$

- In practice, we constrain the 4 highest-order coefficients in a fit using these sum rules by solving a system of equations derived from these sum rules.

FF Uncertainties

- The value of the form factor at some fixed Q^2 is a ***linear*** function of the coefficients, which are the parameters in the fit:

$$G(Q^2;\boldsymbol{a}) = \sum_{k=0}^{k_{\text{max}}} a_k z^k(Q^2) = g + \sum_{k=1}^{k_{\text{max}}} a_k(z^k - z_0^k)\,,$$

  where we used the normalization constraint to re-express the form factor in the second equality, with $z_0 = z(Q^2 = 0; t_0)$ and, e.g., for the proton, $g = (1, \mu_p)$ for the (electric, magnetic) form factors.
- To obtain the uncertainty, we note that

$$\frac{dG}{da_k}(Q^2;\boldsymbol{a}) = z^k - z_0^k\,;$$

  if C_{kl} is the covariance matrix for the coefficients a_k, we have

$$\delta G(Q^2) = \left[\sum_{k,l=1}^{k_{\text{max}}} C_{kl}(z^k - z_0^k)(z^l - z_0^l)\right]^{1/2}.$$

- If a fit includes sum rules, there are straightforward complications to the above derivations.

Datasets

Proton: three separate datasets for the available elastic ep-scattering data.

- **"Mainz" (cross sections)**: high-statistics dataset with $Q^2 < 1.0\,\mathrm{GeV}^2$. Originally 1422 data points in the full dataset released by the A1 collaboration [Bernauer et al. (2014)]. This was rebinned to 658 points with modified uncertainties in Lee et al. (2015).
- **"world" (cross sections)**: compilation of datasets from other experiments from 1966–2005, 569 data points with $Q^2 < 35\,\mathrm{GeV}^2$. Update of dataset used in Arrington et al. (2003, 2007).
- **"pol" (FF ratios)**: 66 polarization measurements with $Q^2 < 8.5\,\mathrm{GeV}^2$, see, e.g., Arrington et al. (2003, 2007), Zhan et al. (2011).

Neutron: the data is split into measurements for G_E^n and G_M^n separately.

- G_E^n: 37 measurements $Q^2 < 3.4\,\mathrm{GeV}^2$.
- G_M^n: 33 measurements $Q^2 < 10\,\mathrm{GeV}^2$.

Ongoing Work

Proton: a combined fit of the three datasets to provide parameterizations and tabulations (including uncertainties) of G_E^p, G_E^n with:

- correlated systematic parameters for the Mainz data floating in the fit,
- implementation of sum rules enforcing dipole-like behaviour of G_E, G_M at high-Q^2,
- updated application of radiative corrections, e.g., high-Q^2 finite two-photon exchange corrections,
- focus on two Q^2 ranges, i.e., $1\text{–}3\,\mathrm{GeV}^2$ and the entire range of available data (up to $35\,\mathrm{GeV}^2$).

Neutron:

- including this data in a combined fit allows us to separate the isoscalar and isovector channels, $G_E^{\binom{0}{1}} = G_E^p \pm G_E^n$, which allows us to move t_{cut} for $G_E^{(0)}$ to the three-pion production threshold, Hill and Paz 2010
- updated determination of neutron electric and magnetic radii.

$k_{\max}$ Dependence

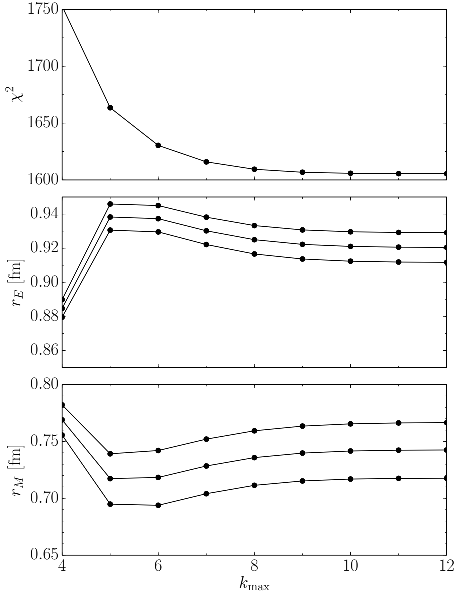

- We can also test the dependence of the fit results on the choice of $k_{\max}$.
- The fit has converged for $k_{\max} = 10$.
- We use a default of $k_{\max} = 12$ in fits: for $Q^2_{\max} = 1.0\,\mathrm{GeV}^2$ (statistics-only errors),

$$r_E = 0.920(9) \text{ fm},$$
$$r_M = 0.743(25) \text{ fm}.$$

Unbounded z Expansion Fits

Fits using unbounded z expansion performed by Lorenz et al. Eur. Phys. J. A48, 151; Phys. Lett. B737, 57

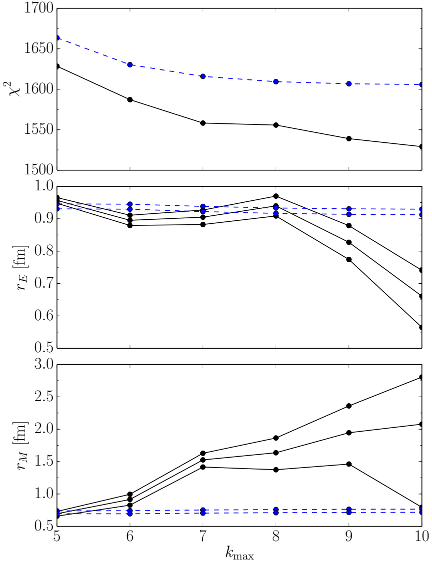

- Sum rules such as ($t_0 = 0$)

$$G_E(q^2 = 0) = \sum_{k=0}^{k_{\text{max}}} a_k = 1$$

  tell us $a_k \to 0$ as the k becomes large.
- The Sachs form factors are also known to fall off as Q^4 up to logs for large Q^2 (dipole-like behaviour at large Q^2).
- To test enlarging the bound, we took $|a_k|_{\text{max}} = |b_k|_{\text{max}}/\mu_p = 10$, and found $r_E = 0.916(11)$ fm, $r_M = 0.752(34)$ fm.
- However, as $|a_k|_{\text{max}} \to \infty$, $|a_k|$ for large k takes on unreasonably large values, in conflict with QCD.

One-Loop $\mathcal{O}(\alpha)$ Radiative Corrections

- The proton form factors are defined from the matrix element of one-photon exchange. A consistent definition of the form factors is required to compare extracted radii.

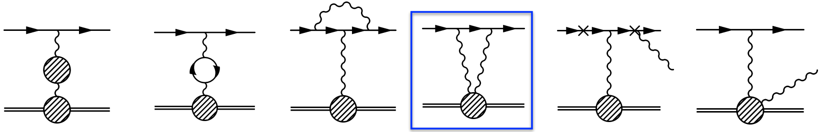

- We know how to compute results for the electron vertex correction and the leptonic contributions to the vacuum polarization in perturbation theory.
- From previous dispersive analyses of $e^+e^- \to$ hadrons data, we expect the correction from hadronic vacuum polarization to be smaller than current achieved precision in scattering experiments. Jegerlehner (1996), Friar et al. (1999)
- For soft bremsstrahlung and two-photon exchange (TPE), there are two conventions for subtraction of infrared divergences. Tsai (1961), Maximon & Tjon (2000)
- At present, we cannot calculate the remainder of the TPE contribution from first principles.

EFT Analysis of Large Logs

A systematic analysis of the radiative corrections using effective field theory is performed by R. Hill in 1605.02613, identifying the sources of all large logarithms in the limit $Q^2 \gg m^2$; e.g., there are implicit conventions of $\mu^2 = M^2$ for vertex corrections vs. $\mu^2 = Q^2$ for Maximon-Tjon TPE corrections.

- Heavy particle: $\Delta E \ll E \sim Q \sim M$. Neglected: $\alpha^2 \log^2(M^2/(\Delta E)^2)$ small.
- Relativistic particle: $m, \Delta E \ll E, Q \ll M$. Neglected: $\alpha^2 \log^3(Q^2/m^2) \sim \mathcal{O}(\alpha^{1/2})$.
- 0.5–1% discrepancies between the NLO resummed EFT prediction and the phenomenological analysis, which is greater than the assumed $< 0.5\%$ systematic error of the A1 analysis.

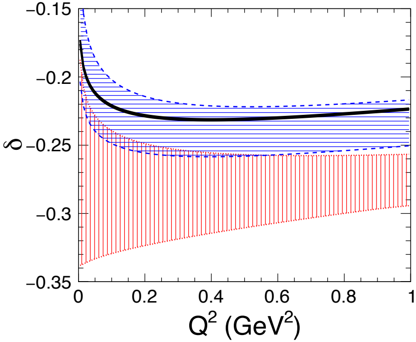

- Leading log resummation.
- Next-to-leading log resummation.
- Black: complete next-to-leading order resummation.
- Bands from varying low and high renormalization scales μ_L^2, μ_H^2 between $1/2 * \min$ and $\Delta E^2, m^2$ and $2 * \max$ of Q^2, E^2.